DALTON
FULL PAPER

Complexes of new chiral terpyridyl ligands. Synthesis and characterization of their ruthenium(II) and rhodium(III) complexes

Marco Ziegler,[a] Véronique Monney,[a] Helen Stoeckli-Evans,[b] Alex Von Zelewsky,*[a] Isabelle Sasaki,[c] Gilles Dupic,[c] Jean-Claude Daran[c] and Gilbert G. A. Balavoine*[c]

[a] *Institut de Chimie Inorganique et Analytique, Université de Fribourg, Pérolles, CH-1700 Fribourg, Switzerland*
[b] *Institut de Chimie, Université de Neuchâtel, Av. Bellevaux 51, CH-2000 Neuchâtel, Switzerland*
[c] *Laboratoire de Chimie de Coordination, CNRS, 205 route de Narbonne, F-31077 Toulouse, France*

Received 6th January 1999, Accepted 12th January 1999

Enantiomerically pure, chiral terpyridyl-type ligands L^1 ('dipineno'-[5,6:5″,6″]-fused 2,2′:6′,2″-terpyridine) and L^2 ('dipineno'-[4,5:4″,5″]-fused 2,2′:6′,2″-terpyridine) have been synthesized in high yields starting from 2,6-diacetylpyridine and enantiopure α-pinene. Complexes of L^1 and L^2 with Rh^{III} and Ru^{II} have been prepared and studied spectroscopically. The complexes $[Ru(L)_2][PF_6]_2$ (L = L^1 or L^2) were obtained in high yields using microwave heating in ethylene glycol as solvent. The rhodium(III) and ruthenium(II) complexes of L^1 and L^2 have a helically distorted terpyridyl moiety, as shown by the considerable optical activity in the ligand centered and metal to ligand charge transfer transitions. Crystal structures of $[Rh(L^1)Cl_3]$ and $[Ru(L^1)Cl_3]$ show a considerable out of plane distortion of the terpyridyl moiety, whereas free L^2 and $[Ru(trpy)(L^2)][PF_6]_2$ have a more planar arrangement of the pyridyl units.

Introduction

Substituted 2,2′:6′,2″-terpyridines are promising building blocks for supramolecular systems[1] and there is great interest in their co-ordination with transition metals,[2–7] mainly due to their interesting photophysical properties[8,9] and potential pharmaceutical applications.[10,11] We report here the synthesis and characterization of "chiralized" 'pineno'-fused terpyridyl ligands $L^1(+)$ and $L^1(-)$ (L^1 = 'dipineno'-[5,6:5″,6″]-fused 2,2′:6′,2″-terpyridine) and $L^2(+)$ and $L^2(-)$ (L^2 = 'dipineno'-[4,5:4″,5″]-fused 2,2′:6′,2″-terpyridine) and their ruthenium(II) complexes, which have predetermined helical twist.† Predetermination of the chirality of metal complexes using chiral ligands is of current interest and has been achieved in our group for bis- and tris-diimine complexes,[13–15] and extended to quaterpyridines[16] using our concept.

With C_2-symmetrical, chiral terpyridyl ligands like L^1 or L^2 three different stereoisomers are possible in an octahedral *mer* arrangement: an enantiomeric pair with D_2 symmetry and an achiral, S_4-symmetrical diastereomer (Scheme 1). In the D_2-symmetrical, octahedral complexes a helical twist is induced by the non-planarity of the ligand. The S_4-symmetrical complex is an example of a "narcissistic coupling"[17a] between two enantiomers giving a *meso* achiral complex. From a purely geometrical point of view it is also possible to divide such an achiral S_4-symmetrical complex by the "coupe du roi"[17b,c] into two homochiral halves, cutting through the metal and the central pyridyl moiety of each ligand, which is, however, impossible in a real molecule.

† The designation $L^1(+)$ refers to the enantiomer obtained from (+)-α-pinene, $L^1(-)$ from (−)-α-pinene, $L^2(+)$ from (+)-myrtenal and $L^2(-)$ from (−)-myrtenal. The locants 5,6:5″,6″ refer to the numbering of the 2,2′:6′,2″-terpyridyl moiety and indicate the fusion sites with the 'pinene' moiety. This numbering scheme was introduced for related ligands.[12] L^1 = 2,6-Bis(6,6-dimethyl-5,6,7,8-tetrahydro-5,7-methanoquinolin-2-yl)pyridine, L^2 = 2,6-bis(7,7-dimethyl-5,6,7,8-tetrahydro-6,8-methanoisoquinolin-3-yl)pyridine.

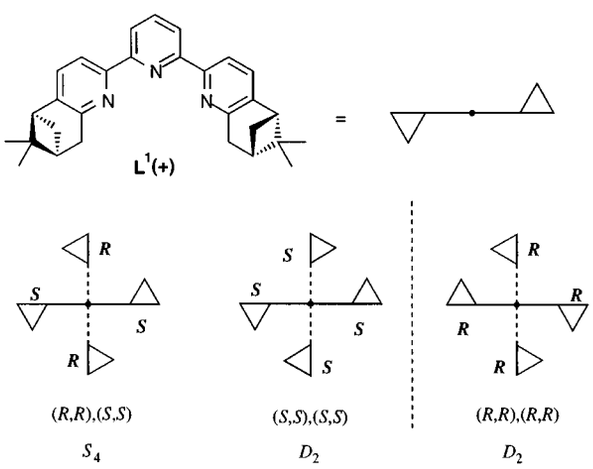

Scheme 1 Possible arrangements of octahedral complexes with chiral terpyridyl type ligands.

Experimental

Synthetic methods

The enantiomerically pure ligands L^1 and L^2 have been obtained in an analogous preparation to the "CHIRAGEN" ligand system[15] according to Scheme 2. Complexes were synthesized according to Scheme 3; $[Ru(trpy)Cl_3]$ was prepared following literature methods.[18,19]

Preparations

(1*S*)-(−)-Pinocarvone (6,6-dimethyl-2-methylenebicyclo-[3.1.1]heptan-3-one) I. Following the literature procedure,[20] compound **I** was obtained in 85–100% yields from (1*R*)-(+)-α-pinene [enantiomeric excess, e.e.: 98%. α (589 nm, 21 °C) = 50.7°] as starting material. (1*R*)-(+)-Pinocarvone **II** was obtained

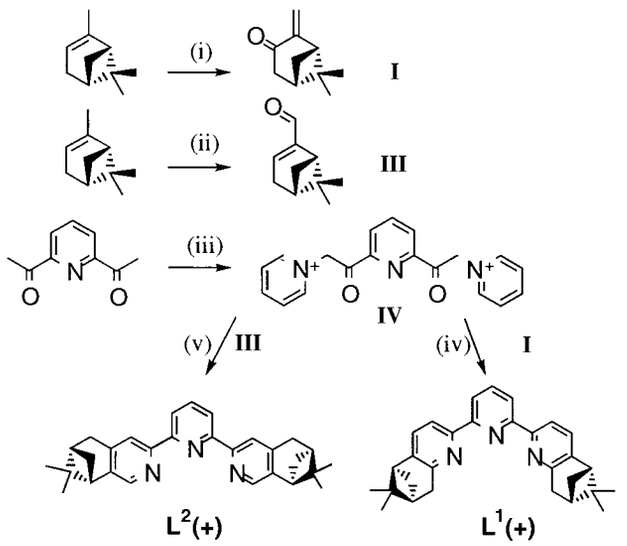

Scheme 2 (i) $^1O_2$, Acetic anhydride, DMAP, [(4-dimethylamino)-pyridine] CH_2Cl_2, TPP, (5,10,15,20-tetra phenyl porphyrin) 20 °C, 8 h;[20] (ii) SeO_2, *t*-BuOOH, CH_2Cl_2, 35 °C, 48 h;[21] (iii) I_2/py; (iv) ammonium acetate, acetic acid, 125 °C, 12 h; (v) ammonium acetate, acetic acid, formamide, 100 °C, 12 h.

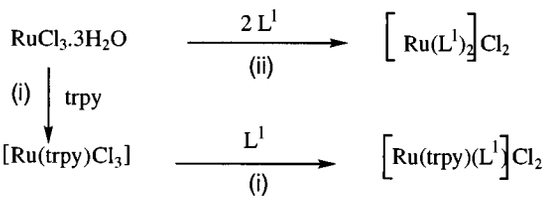

Scheme 3 (i) EtOH–water, 2–12 h, 80 °C; (ii) CH_2OHCH_2OH, 4 min, microwave heating, 375 W.

from (1*S*)-(−)-α-pinene [e.e.: 98%. *α* (589 nm, 21 °C) = −50.1°] using the same procedure.

(1*S*)-(+)-Myrtenal (6,6-dimethylbicyclo[3.1.1]hept-2-ene-2-carbaldehyde) III. This was obtained in 32% yield from (1*R*)-(+)-α-pinene after silica gel chromatography using ethyl acetate–hexane (10:90) as the eluent following a literature procedure.[21] The pure product was characterized by ^{1}H NMR. (1*R*)-(−)-Myrtenal is commercially available.

2,6-Bis(pyridinioacetyl)pyridine diiodide IV. To a solution of 3.27 g (20 mmol) of 2,6-diacetylpyridine (Fluka purum) in 15 mL of dry pyridine was added a solution of 10.45 g (41 mmol) of sublimated iodine in 15 mL of dry pyridine. The mixture was heated at 100 °C for 3 h and after cooling, the precipitate is filtered off, rinsed once with pyridine and dried. Recrystallization from 95% ethanol yielded 9.71 g of a beige powder (91%). ^{1}H NMR (DMSO-d_6): δ 9.12 [d, 4 H, H(10), $^3J(H^{10}H^{11}) = 5.7$]; 8.79 [dd, 2 H, H(12), $^3J(H^{12}H^{11}) = 7.8$]; 8.44 [s, 3 H, H(4), H(5)]; 8.34 [dd, 4 H, H(11), $^3J(H^{11}H^{12}) = 7.8$, $^3J(H^{11}H^{10}) = 5.7$ Hz] and 6.71 [s, 4 H, H(8)]. MS(EI): *m*/*z* 446 ($M^+ - I^-$); 318 ($M^+ - 2I^- - H^+$) and 240 ($M^+ - 2I^- -$ py) (Found: C, 38.08; H, 2.88; N, 6.92. Calc. for $C_{19}H_{17}I_2N_3O_2 + H_2O$: C, 38.60; H, 3.2; N, 7.10%) Crystal data: $C_{19}H_{17}I_2N_3O_2$], $M = 826.96$, orthorhombic, space group *Pbca*, $a = 11.253(4)$, $b = 16.741(4)$, $c = 25.941(7)$ Å, $U = 4887(3)$ Å^3, $Z = 8$, $D_c = 2.249$ g cm^{-3}, $T = 293(2)$ K, 4687 reflections measured, 3387 unique ($R_{int} = 0.0332$) of which all were used in all calculations; final $wR(F)$ 0.0402, goodness of fit 1.020.

L^1(−). Compound **II** (9.0 g, 0.060 mol) **2**, 17.2 g (0.030 mol) of **IV**, and 9.24 g ammonium acetate (0.120 mol, Merck p.a.) were dissolved in 100 mL glacial acetic acid, refluxed overnight, and 100 mL water added to the ice cold solution. The solution was extracted four times with 150 mL diethyl ether. The extracts were combined and washed first with 70 mL water, then four times with saturated $NaHCO_3$ solution and finally with saturated NaCl. After drying over $MgSO_4$ and filtration over active carbon the product slowly crystallized by evaporation of the solvent (8.84 g, 70%). The compound L^1(+) was prepared similarly in 62% yield. ^{1}H NMR ($CDCl_3$): δ 8.37 [d, 2 H, H(12), $^3J(H^{12}H^{11}) = 7.9$]; 8.28 [d, 2 H, H(3), H(5), $^3J(H^3H^4) = 7.7$]; 7.88 [dd, 1 H, H(4), $^3J(H^4H^3) = 7.8$]; 7.34 [d, 2 H, H(11), $^3J(H^{11}H^{12}) = 7.8$]; 3.20 [d, 4 H, H(13a/13b), $^3J(H^{13}H^{14}) = 2.6$]; 2.81 [dd, 2 H, H(16), $^3J(H^{16}H^{15b}) = 5.6$, $^4J_{16,14} = 5.6$]; 2.70 [dd, 2 H, H(15b), $^3J(H^{15b}H^{14}) = 5.6$, $^3J(H^{15b}H^{16}) = 5.6$, $^2J_{15b,15a} = 9.6$]; 2.40 [m sept, 2 H, H(14)]; 1.41 [s, 6 H, H(19)]; 1.31 [d, 2 H, H(15a), $^2J_{15a,15b} = 9.6$]; and 0.68 [s, 6 H, H(18)]. ^{13}C-{^{1}H} NMR ($CDCl_3$): δ 156.3, 153.8, 142.2, 137.6, 133.7, 120.1, 177.9, 46.6, 40.3, 39.6, 36.7, 32.0, 26.1 and 21.3 (Found: C, 81.97; H, 7.59; N, 9.73. Calc. for $C_{29}H_{31}N_3$: C, 82.62; H, 7.41; N, 9.97%). MS(EI): *m*/*z* 421 (100, M^+); 406 (38, $M^+ - CH_3$); 380 (46, $M^+ - H_2C=C^+-CH_3$); 334 (26); 167 (61); 128 (20); 77 (22); and 43 (73%). *α* (330 nm) = −80 °C, *α* (370) = −65 °C [20 °C, $c = 8 \times 10^{-5}$ M (1.68 mg in 50 mL acetonitrile)].

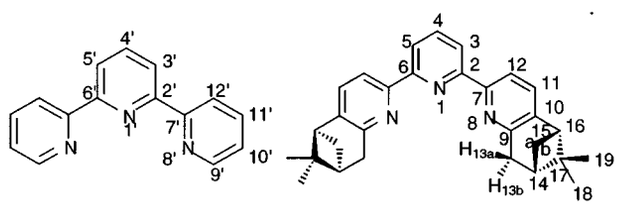

L^2(+). To a solution of 2.89 g (5.03 mmol) of compound **IV** in formamide were added 1.66 g (21.5 mmol) of ammonium acetate and 1.52 g (10.1 mmol) of **III**. Heating at 80 °C was maintained overnight. The precipitate was filtered off, rinsed with water and dried. It could be used without purification for the synthesis of the complexes or recrystallized from ethyl acetate (yield = 36%). Compound L^2(−) was prepared similarly from (1*R*)-(−)-myrtenal in 64% yield. ^{1}H NMR ($CDCl_3$): δ 8.37 (s, 2 H), 8.34 (d, 2 H, $^3J = 7.8$), 8.21 (s, 2 H), 7.90 (t, 1 H, $^3J = 7.7$), 3.11 (d, 4 H, $^3J = 2.7$), 2.88 (dd, 1 H, $^3J = 5.5$, $^4J = 5.5$), 2.68 (ddd, 2 H, $^2J = 9.5$, $^3J = 5.7$, 5.4), 2.34 (m sept, 2 H), 1.42 (s, 6 H), 1.25 (d, 2 H, $^2J = 9.5$ Hz) and 0.67 (s, 6 H). ^{13}C-{^{1}H} NMR ($CDCl_3$): δ 155.82, 154.63, 145.49, 145.30, 142.92, 137.70, 120.46, 120.36, 44.51, 40.12, 39.25, 33.03, 31.83, 26.01 and 21.38. IR (KBr): 2923m, 1709 (s), 1554m, 1455m and 1385m (Found: C, 82.72; H, 7.50; N, 9.88. Calc. for $C_{29}H_{31}N_3$: C, 82.62; H, 7.41; N, 9.97%). MS (DCI, NH_3): *m*/*z* = 422 $[M + H]^+$. *α* (589 nm, 20 °C, 9.6 mg in 2 mL of $CHCl_3$) = +163.5°.

[Ru(trpy)$_2$][PF$_6$]$_2$ 1. In a 100 mL round flask, 117 mg (0.5 mmol) trpy (Fluka, purum) and 65.5 mg $RuCl_3 \cdot 3H_2O$ (0.25 mmol) were suspended in 4 mL ethylene glycol (Fluka, purum) and refluxed for 4 min in a microwave oven (325 W). The salt NH_4PF_6 (1.0 g) in 25 mL water was added to the orange-brown solution, the precipitate collected in a Buchner funnel, washed with water and a little diethyl ether and recrystallized from acetonitrile–diethyl ether. Yield: 190.5 mg (89%). ^{1}H NMR (CD_3CN): δ 8.73 [d, 4 H, H(3), $^3J(H^3H^4) = 8.1$]; 8.47 [d, 4 H, H(12), $^3J(H^{12}H^{11}) = 8.5$]; 8.39 [dd, 2 H, H(4), $^3J(H^4H^3) = 8.0$]; 7.90 [td, 4 H, H(11), $^3J(H^{11}H^{12}) = 7.8$, $^4J(H^{11}H^9) = 1.5$]; 7.32 [d, 4 H, H(9), $^3J(H^9H^{10}) = 5.2$]; 7.14 [ddd, 4 H, H(10), $^3J(H^{10}H^{11}) = 7.8$, $^3J(H^{10}H^9) = 5.6$, $^4J(H^{10}H^{12}) = 1.4$ Hz]. MS(EI): *m*/*z* 713 (15, $M^+ - PF_6$); 567 (22, $M^+ - 2\ PF_6$); 334 (20); 234 (100); and 154 (100%).

DC: silica gel; DMF: 8; H_2O: 5 EtOH: 3; NaCl: 0.3 M; NH_4Cl: 0.2 M; $R_f = 0.58$.

[Ru(L^1)(−)Cl_3 2. The compound L^1(−) (84.3 mg, 0.2 mmol) and 48.6 mg $RuCl_3 \cdot 3H_2O$ (0.2 mmol) were suspended in 10 mL 1-butanol (Fluka, puriss.) and kept under constant reflux for 12 h. The greenish powder was filtered off and washed with a little diethyl ether. Drying to constant weight yielded 115 mg of a green-brownish powder (92%). The substance was paramagnetic and contained some $[Ru(L^1(-))_2]Cl_2$. Recrystallization from acetone yielded small, needle like crystals of **2**. Diluted solutions of it in a number of polar solvents (EtOH, DMF, DMSO) all contained dissociated Ru^{III} and free L^1(−) as seen from the precipitation of the latter after slow evaporation and from spectroscopic data. MS(EI): *m*/*z* 593 (32, $M^+ - Cl$); 557 (28, $M^+ - 2\ Cl$); and 518 (100, $M^+ - 3\ Cl$).

[Rh(L^1(−))Cl_3 3. In a 100 mL round flask, 1.60 g (3.80 mmol) L^1(−) and 1.00 g $RhCl_3 \cdot 3H_20$ were refluxed for 4 h in 30 mL ethanol. The orange-red precipitate was filtered off, washed with a little ethanol and recrystallized from dichloromethane–diethyl ether (153 mg, 94%). The complex $[Rh(L^1(+))Cl_3]$ **4** was obtained similarly from L^1(+) in 87% yield. ^{1}H NMR ($CDCl_3$): δ 8.03 [s, 3 H, H(3), H(4), (H5)]; 7.83 [d, 2 H, H(12), $^3J(H^{12}H^{11}) = 7.8$]; 7.44 [d, 2 H, H(11), $^3J(H^{11}H^{12}) = 7.8$]; 4.46 [m large, 4 H, H(13)]; 2.82 [dd, 2 H, H(16), $^3J(H^{16}H^{15b}) = 5.7$, $^4J(H^{16}H^{14}) = 5.7$]; 2.61 [dd, 2 H, H(15b), $^3J(H^{15b}H^{14}) = 5.7$, $^3J(H^{15b}H^{16}) = 5.7$, $^2J(H^{15b}H^{15a}) = 9.9$]); 2.47 [m sept, 2 H, H(14)]; 1.38 [s, 6 H, H(19)]; 1.28 [d, 2 H, H(15a), $^2J(H^{15a}H^{15b}) = 9.9$ Hz]; and 0.68 [s, 6 H, H(18)]. MS(FAB): *m*/*z* 594 (100); 595 (34); 596 (69); 597 (22); 598 (14); 599(4) ($M^+ - Cl$); 559 (100); 560 (34); 561 (37); 562 (11); and 563 (1%) ($M^+ - 2\ Cl$). UV-VIS (CH_2Cl_2, $c = 2.00 \times 10^{-5}$ M): λ/nm (ε/M^{-1} cm^{-1}) 242 (42570); 276 (sh, 17000); 312 (21900); 354 (18000) and 376 (sh, 7600). α [404.6 nm, 20 °C, $c = 2.00 \times 10^{-5}$ M (0.630 mg in 50 mL dichloromethane] = +1250°.

[Ru(trpy)(L^1(−)][PF_6]$_2$ 5. The complex $[Ru(trpy)Cl_3]$ (147 mg, 0.33 mmol) and 140 mg (0.33 mmol) L^1(−) were refluxed in 15 mL ethylene glycol under vigorous stirring for 1 h. The solvent was distilled off and the black residue dissolved in 100 mL water. After removal of unreacted complex by filtration the product was precipitated upon addition of 0.78 g NH_4PF_6 and filtered off. Washing twice with 10 mL CH_2Cl_2 and once with 10 mL and drying to constant weight yielded 235 mg of an orange powder (67%). Recrystallization from a variety of solvents yielded needle like intense red crystals of **5** that were, however, unsuitable for X-ray measurements. ^{1}H NMR (CD_3CN): δ 8.71 [d, 2 H, H(3), $^3J(H^3H^4) = 8.2$]; 8.63 [d, 2 H, H(3′), $^3J(H^{3'}H^{4'}) = 8.2$]; 8.48 [ddd, 2 H, H(12′), $^3J(H^{12'}H^{11'}) = 8.1$, $^4J(H^{12'}H^{10'}) = 0.8$, $^5J_{12',9'} = 0.6$]; 8.39 [t, 1 H, H(4′), $^3J(H^{4'}H^{3'}) = 7.9$]; 8.34 [t, 1 H, H(4), $^3J(H^4H^3) = 7.9$]; 8.24 [d, 2 H, H(12), $^3J(H^{12}H^{11}) = 8.0$]; 7.93 [td, 2 H, H(11′), $^3J(H^{11'}H^{10'}) = 7.9$, $^4J(H^{11'}H^{9'}) = 1.5$]; 7.58 [dd, 2 H, H(9′), $^3J(H^{9'}H^{10'}) = 5.8$]; 7.43 [d, 2 H, H(11), $^3J(H^{11}H^{12}) = 8.0$]; 7.27 [ddd, 4 H, H(10′), $^3J(H^{10'}H^{11'}) = 7.9$, $^3J(H^{10'}H^{9'}) = 5.7$, $^4J(H^{10'}H^{12'}) = 1.4$]; 2.63 [t, 2 H, H(16), $^3J(H^{16}H^{15b}) = 5.7$, $^4J(H^{16}H^{14}) = 5.7$]; 2.31 [ddd, 2 H, H(15b), $^2J(H^{15b}H^{15a}) = 9.6$, $^3J(H^{15b}H^{14}) = 5.3$, $^3J(H^{15b}H^{16}) = 5.4$]; 1.79 [dd, 2 H, H(13b), $^2J(H^{13b}H^{13a}) = 16.7$, $^4J(H^{13b}H^{14}) = 2.9$]; 1.71 [m, 2 H, H(14)]; 1.67 [dd, 2 H, H(13a), $^2J(H^{13a}H^{13b}) = 16.4$, $^4J(H^{13b}H^{14}) = 3.0$]; 1.13 [s, 6 H, H(19)]; [0.70 (d, 2 H, H(15a), $^2J(H^{15a}H^{15b}) = 9.9$ Hz]; and −0.14 [s, 6 H, H(18)]. NOE (300 MHz, acetonitrile): δ 2.63 (1.9 {1.13}); 2.31 (0.6 {1.71}, 2.61 {1.13}); 1.71 (1.6 {1.13}); 1.13 (0.8 {1.71}); 0.70 (1.0 {1.71}; −0.14 (2.7 {1.13}, 2.0% {1.71}). MS(EI): *m*/*z* 902 (20, $M^+ - PF_6$); 756 (38, $M^+ - 2\ PF_6$); 422 (80); 334 (32); 154 (100); and 136 (91%). α (404.6 nm) = 520°, α (365 nm) = +1000° [20 °C, $c = 1.017 \times 10^{-4}$ M (5.32 mg in 50 mL acetonitrile)].

DC: silica gel; DMF: 8; H_2O: 5 EtOH: 3; NaCl: 0.3; NH_4Cl: 0.2; $R_f = 0.72$.

[Ru(L^1(−))$_2$][(PF_6]$_2$ 6. In a 50 mL round flask, 32.8 mg (0.125 mmol) $RuCl_3 \cdot 3H_2O$ and 105.4 mg (0.25 mmol) L^1(−) were suspended in 3 mL ethylene glycol (Fluka, purum) and refluxed for 4 min in a microwave oven (325 W). The salt NH_4PF_6 (0.5 g) in 20 mL water was added to the deep red, brownish solution, the precipitate collected in a Buchner funnel, washed with water and a little diethyl ether and recrystallized from acetonitrile–diethyl ether (153 mg, 99%). In another attempt under the same reaction conditions, 53.4 mg (95%) of $[Ru((L^1(+))_2][BPh_4]_2$ were obtained after recrystallization from acetone–pentane starting with 29.9 mg L^1(+) and precipitation with $NaBPh_4$. ^{1}H NMR (CD_3CN): δ 8.61 [d, 2 H, H(3), H(5), $^3J(H^3H^4) = 7.7$]; 8.32 [dd, 1 H, H(4), $^3J(H^4H^3) = 7.8$]; 8.25 [d, 2 H, H(12), $^3J(H^{12}H^{11}) = 7.9$]; 7.46 [d, 2 H, H(11), $^3J(H^{11}H^{12}) = 7.8$]; 2.69 [dd, 2 H, H(16), $^3J(H^{16}H^{15b}) = 5.2$, $^4J(H^{16}H^{14}) = 5.2$]; 2.34 [ddd, 2 H, H(15b), $^3J(H^{15b}H^{14}) = 5.6$, $^3J(H^{15b}H^{16}) = 5.6$, $^2J(H^{15b}H^{15a}) = 9.6$]; 2.01 [d, 4 H, H(13a/13b), $^3J(H^{13}H^{14}) = 2.1$]; 1.78 [m sept, 2 H, H(14)]; 1.16 [s, 6 H, H(19)]; 0.84 [d, 2 H, H(15a), $^2J(H^{15a}H^{15b}) = 9.8$ Hz];and −0.14 [s, 6 H, H(18)]. NOE (300 MHz, acetonitrile): δ 8.61 (25.4 {8.25}, 1.2 {2.01}); 8.25 (0.7 {2.01}); 7.46 (9.4 {8.25}, 12.2 {2.69}, 0.5 {2.01}); 2.34 (1.0 {2.69}); 1.16 (3.6 {2.69}); 0.84 (1.0 {2.69}, 1.6 {2.01}); and −0.14 (0.8 {2.69}, 3.5% {2.01}). MS(EI): *m*/*z* 1090 (42, $M^+ - PF_6$); 944 (79, $M^+ - 2\ PF_6$); 518 (42); 472 (50); 154 (100); 136 (>100%). α (404.6 nm) = +1430°, α (365 nm) = +2580° [20 °C, $c = 7.29 \times 10^{-5}$ M (4.50 mg in 50 mL acetonitrile)].

DC: silica gel; DMF: 8; H_2O: 5 EtOH: 3; NaCl: 0.3; NH_4Cl: 0.2; $R_f = 0.80$.

[Ru(trpy)(L^2(+))]Cl_2 7. The complex $[Ru(trpy)Cl_3]$ (74 mg) and 70 mg of L^2(+) were refluxed in 20 mL of EtOH–water (1 : 1) for 1 d. The solvent was evaporated and the dark residue dissolved in 2 mL of 95% ethanol. After filtration of insoluble material the filtrate was purified by chromatography on a Sephadex LH20 column. The complex was eluted with 95% EtOH and after evaporation of the solvent the product was recovered as an red-orange powder (yield: 66%). The complex $[Ru(trpy)(L^2(-))]Cl_2$ **8** has been obtained similarly in 76% yield. ^{1}H NMR (CD_3OD): δ 8.96 (d, 2 H, $^3J = 8.1$), 8.88 (d, 2 H, $^3J = 8.1$), 8.72 (d, 2 H, $^3J = 8.1$), 8.55 (s, 2 H), 8.46 (t, 2 H, $^3J = 8.1$), 8.01 (dt, 2 H, $^3J = 7.9$, $^4J = 1.4$), 7.49 (dd, 2 H, $^3J = 5.4$, $^4J = 0.6$), 7.30 (dt, 2 H, $^3J = 6.2$, $^4J = 1.1$), 6.92 (s, 2 H), 3.21 (d, 4 H, $^3J = 2.3$), 2.62 (m, 2 H), 2.56 (dd, 2 H, $^3J = 5.6$, $^4J = 5.6$), 2.28 (m, 2 H), 1.29 (s, 6 H), 0.98 (d, 2 H, $^3J = 8.9$ Hz) and 0.38 (s, 6 H). ^{13}C-{^{1}H} NMR (CD_3OD): δ 159.93, 157.80, 157.24, 157.05, 153.32, 149.75, 149.53, 148.31, 139.40, 137.53, 137.14, 129.09, 125.97, 125.55, 125.27, 124.18, 45.82, 41.03, 39.91, 34.19, 31.98, 26.10 and 21.50. FAB (3-nitrobenzyl alcohol): *m*/*z* = 791, $[M - Cl]^+$; and 756, $[M - 2\ Cl]^+$ (Found: C, 55.46; H, 5.78; N, 8.85. Calc. for $C_{44}H_{42}Cl_2N_6Ru + 7\ H_2O$: C, 55.46; H, 5.88; N, 8.82%). α (589 nm, 20 °C, 0.146 mg in 2 mL of EtOH) = +274°. $[Ru(trpy)(L^2(-))][PF_6]_2$ **8a** was prepared for X-ray analysis.

[Ru(L^2(+))$_2$]Cl_2 9. To 30 mg (0.14 mmol) of $RuCl_3 \cdot 3H_2O$ in 20 mL of EtOH–water (1 : 1) were added 130 mg (0.31 mmol) of L^2(+) and refluxed for 1 d. After evaporation of the solvent the mixture was purified on Sephadex LH20 as described. The complex $[Ru(L^1(-))_2]Cl_2$ **10** was prepared similarly from L^2(−) in 56% yield. Quantitative yields were obtained by microwave heating (4 min, 375 W) in ethylene glycol using the same procedure as for $[Ru(L^1)_2][PF_6]_2$. ^{1}H NMR (CD_3OD): δ 8.85 (d, 4 H, $^3J = 8.1$), 8.52 (s, 4 H), 8.41 (t, 2 H, $^3J = 8.2$), 6.91 (s, 4 H), 3.21 (d, 8 H), 2.64 (m, 4 H), 2.56 (dd, 4 H, $^3J = 5.6$, $^4J = 5.6$), 2.29 (m, 4 H), 1.30 (s, 12 H), 1.23 (d, 4 H, $^3J = 9.6$ Hz) and 0.29 (s, 12 H). ^{13}C-{^{1}H} NMR (CD_3OD): δ 157.83, 157.13, 149.37, 149.29, 148.08, 137.01, 125.40, 124.14, 41.07, 39.94, 34.19, 31.89, 26.04 and 21.44. FAB (3-nitrobenzyl alcohol): *m*/*z* = 979, $[M - Cl]^+$; and 944 $[M - 2\ Cl]^+$ (Found: C, 60.66; H, 6.87; N, 7.14. Calc. for $C_{58}H_{62}Cl_2N_6Ru + 7\ H_2O$: C, 61.05; H,

Table 1 Shifts of protons of the unsubstituted trpy unit upon complexation in $[Ru(trpy)_2]^{2+}$ and in $[Ru(trpy)(L^1(-))]^{2+}$. The solvent for the complexes is CD_3CN. For free trpy $CDCl_3$ was used as solvent

	3′	4′	9′	10′	11′	12′
trpy	8.44	7.94	8.68	7.31	7.84	8.60
$[Ru(trpy)_2]^{2+}$	8.73	8.39	7.32	7.14	7.90	8.47
$\Delta\delta$	*+0.29*	*+0.45*	*−1.36*	*−0.17*	*+0.06*	*−0.13*
$[Ru(trpy)(L^1)]^{2+}$	8.63	8.39	7.58	7.27	7.93	8.48
$\Delta\delta$	*+0.19*	*+0.45*	*−1.10*	*−0.04*	*+0.09*	*−0.12*

6.66; N, 7.37%). *a* (589 nm, 20 °C, 0.226 mg in 2 mL of EtOH) = +504°.

$[Ru(L^1(-))(L^1(+))][PF_6]_2$ 11. This was obtained from $[Ru(L^1(-))Cl_3]$ by adding $L^1(+)$ in equimolar amounts using ethylene glycol and microwave heating. However, the product was obtained as a statistical mixture of $[Ru(L^1(-))_2][PF_6]_2$, $[Ru(L^1(+))_2][PF_6]_2$ and $[Ru(L^1(-)(L^1(+))][PF_6]_2$ (1 : 1 : 2). Other solvents with milder conditions (refluxing in EtOH–water) always led to the statistical mixture. Separation of the diastereomers was unsuccessful. ^{1}H NMR (CD_3CN): δ 8.61 [d, 2 H, H(3)]; 8.31 [dd, 1 H, H(4)]; 8.26 [d, 2 H, H(12)]; 7.48 [d, 2 H, H(11)]; 2.69 [dd, 2 H, H(16)]; 2.35 [ddd, 2 H, H(15b)]; 2.01 [d, 4 H, H(13a/13b)]; 1.78 [m sept, 2 H, H(14)]; 1.15 [s, 6 H, H(19)]; 0.61 [d, 2 H, H(15a)]; and −0.01 [s, 6 H, H(18)].

X-Ray crystallography

Details of the crystal parameters, data collection and refinement are given in Table 6. The structures were solved by direct methods and refined by the full-matrix least-squares method on all *F* data, except for $[Rh(L^1(-))Cl_3]$ which was refined on all F^2 with an extinction correction to all F_c data. No absorption corrections were applied for $[Ru(L^1(-))Cl_3]$ and $[Ru(trpy)(L^2(-))][PF_6]_2$ For $[Rh(L^1(-))Cl_3]$ no suitable ψ scans could be measured, and only one equivalent of data was obtained. With $\mu = 1.02$ mm^{-1} and a reasonably low residual electron density (1.162/−1.011 e A^3) no absorption correction was applied. All crystals were stable during the measurements. The H atoms were located on Fourier difference maps, but introduced in idealized positions [d(CH) = 0.96 Å] and their atomic coordinates recalculated after each cycle. They were given isotropic thermal parameters 20% higher than those of the carbon to which they are attached. The absolute configurations for all resolved compounds were examined by refining Flack's parameter *x*. The absolute configuration cannot be determined reliably for $L^2(-)$, whereas for all other compounds the *x* value is in accord with the absolute configuration expected from the synthetic route.

CCDC reference number 186/1310.

See http://www.rsc.org/suppdata/dt/1999/667/ for crystallographic files in .cif format.

Apparatus and chemicals used

For the synthesis of reactants solvents of Fluka *purum* grade quality were used without further treatment. For spectroscopic purposes, acetonitrile from Aldrich (puriss. for spectroscopy) was used. The compound $RuCl_3 \cdot 3H_2O$ (Johnson Matthey) was used as ruthenium source. The NMR spectra were recorded using Bruker AM-250 (250 MHz), Varian Gemini300 (300 MHz) and Bruker DRX500 (500 MHz) spectrometers. The chemical shift values are reported relative to tetramethylsilane. The 2-D COSY and heteronuclear correlation (HETCOR) spectra as well as NOE were obtained according to standard procedures, MS (FAB) spectra on a VG Instruments 7070E spectrometer or with a quadripolar Nermag R10-10H instrument (3-nitrobenzyl alcohol matrix). Elemental analyses were performed by LCC (Laboratoire de Chimie de Coordination) Microanalytical Service. The UV-VIS absorption was determined using a Perkin-Elmer Lambda 5 spectrophotometer with 1 cm quartz cells. Column chromatography purification was performed with 70–200 mm Silica gel or on Sephadex LH20 (Pharmacia). For thin layer chromatography silica gel plates (Merck 60 F_{254}) were used. Optical rotations were measured on a Perkin-Elmer polarimeter 241. The CD spectra were measured on a Dichrograph Mark 5 from Yobin Ivon in a 1 cm quartz cell. Crystal structures were measured on Stoe IPDS and on Stoe-Siemens four-circle AED-2 diffractometers (graphite-monochromated Mo-Kα radiation).

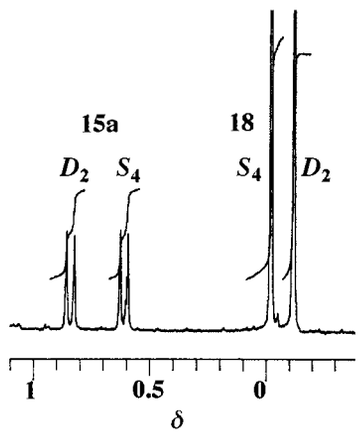

Fig. 1 The NMR signals of a statistical mixture of D_2 and S_4 symmetric $[Ru(L^1)_2][PF_6]_2$ for the aliphatic protons 15a and 18.

Results and discussion

Synthesis

The Kröhnke condensation[22] of chiral β-unsaturated ketones or aldehydes opens an efficient way to chiral terpyridines and their metal complexes. Microwave heating afforded quantitatively bis(terpyridyl)ruthenium(II) complexes of high purity, with typical heating times of only 2–4 min. This procedure shows great advantages over previously reported synthetic methods for the preparation of such complexes in boiling aqueous ethanol.[23–25] As an example, for the preparation of $[Ru(trpy)_2][PF_6]_2$ the yield decreased from 86 (ethylene glycol, 4 min, 375 W) to 65 (ethanol, 3 h) or 21% (DMF, 3 h). It is known that pineno-fused bipyridines can be linked stereoselectively[12,27] by formally substituting H(13). Methylation of $L^1(-)$ yields only one diastereoisomer. Ligands of this type are presently being studied and will be reported elsewhere.

NMR

Table 1 shows relevant protons of the trpy unit with their chemical shifts for the 'free' and complexed ligand in $[Ru(trpy)_2]^{2+}$ and in $[Ru(trpy)(L^1(-))]^{2+}$. The chemical shift of certain protons is highly diagnostic for their environment. In $[Ru(trpy)_2]^{2+}$ the proton 9′ lies above the plane of the central pyridine ring of the other orthogonal ligand and is thus shifted upfield. In $[Ru(trpy)(L^1(-))]^{2+}$ the shielding is less efficient, which may indicate that proton 9′ is pushed away from the face of the opposing central pyridine ring, probably due to the

Table 2 Shifts of protons of free $L^1(-)$ as compared with those of $[Ru(L^1(-))_2]^{2+}$, $[Ru(trpy)(L^1(-))]^{2+}$ and $[Ru(L^1(-)(L^1(+))]^{2+}$; CD_3CN was used as solvent

	3	4	13a/b	14	15a	15b	16	18	19
$L^1(-)$	8.28	7.88	3.20	2.40	1.31	2.70	2.81	0.68	1.41
$[Ru(trpy)(L^1(-))]^{2+}$	8.71	8.34	1.73	1.71	0.70	2.31	2.63	−0.14	1.13
$\Delta\delta$	*+0.43*	*+0.46*	*−1.47*	*−0.69*	*−0.61*	*−0.39*	*−0.18*	*−0.82*	*−0.28*
$[Ru(L^1(-))_2]^{2+}$	8.61	8.32	2.01	1.78	0.84	2.34	2.69	−0.14	1.16
$\Delta\delta$	*+0.33*	*+0.44*	*−1.15*	*−0.62*	*−0.57*	*−0.36*	*−0.12*	*−0.82*	*−0.25*
$[Ru(L^1(-)(L^1(+))]^{2+}$	8.61	8.31	2.01	1.78	0.61	2.35	2.69	−0.01	1.15
$\Delta\delta$	*+0.33*	*+0.43*	*−1.15*	*−0.62*	*−0.70*	*−0.35*	*−0.12*	*−0.69*	*−0.26*

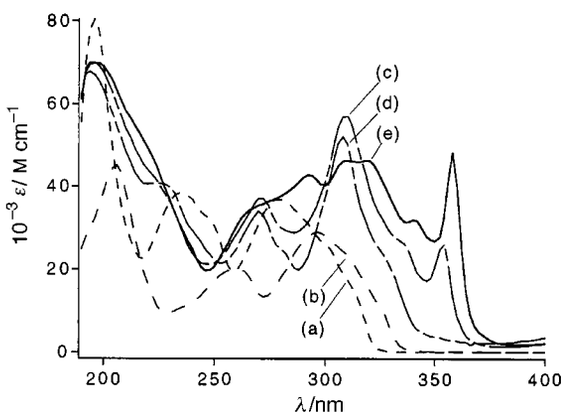

Fig. 2 Ligand centered absorption of trpy (a), $L^1(-)$ (b), $[Ru(trpy)(L^1(-))]^{2+}$ (c), $[Ru(trpy)_2]^{2+}$ (d), and $[Ru(L^1(-))_2]^{2+}$ (e) in acetonitrile (1×10^{-5} M).

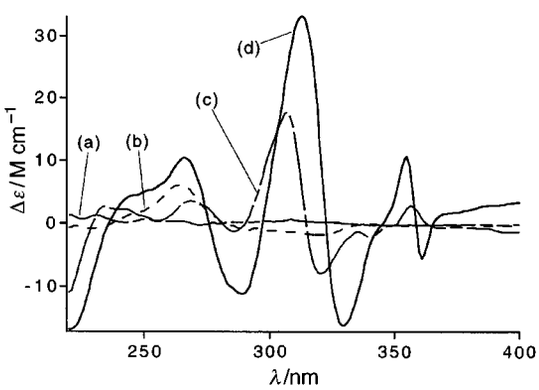

Fig. 3 The CD-spectra of trpy (a), $L^1(-)$ (b), $[Ru(trpy)(L^1(-))]^{2+}$ (c) and $[Ru(L^1(-))_2]^{2+}$ (d) in acetonitrile (1×10^{-5} M).

crowding of the pinene groups of the other ligand. The protons 3′ and 4′ are slightly shifted downfield upon complexation due to their position in the deshielding plane of the two terminal pyridine rings of the orthogonal ligand. The protons 13a/b, 14, 15a/b, 18 and 19 of $L^1(-)$ lie above the plane of the central aromatic pyridine ring and are therefore considerably shifted upfield (Table 2, Fig. 1). In a 1:1 complex the protons 13a/b, 15a/b and 19, however, would not be so much shifted as compared to those of the 2:1 complex. This is clearly the case for $[Rh(L^1(-))Cl_3]$. For the complex $[Ru(trpy)(L^2(+))]^{2+}$ the chemical shifts of the aliphatic protons of L^2 are much closer to those of free L^2 and the upfield shift is less pronounced due to the fact that the pinene group will not come close to the deshielding plane of the orthogonal pyridyl moiety.

Electronic spectra

The electronic spectra of all complexes (Figs. 2–5, Table 4) are characterized by intense absorptions between 200 and 380 nm attributed to $\pi \longrightarrow \pi^*$ transitions associated with the aromatic rings of the ligand. Metal to ligand charge transfer (MLCT)

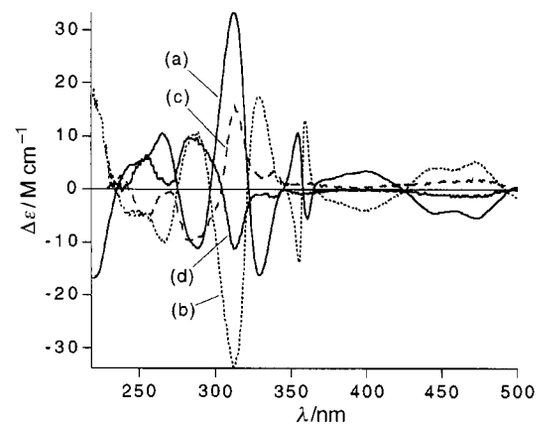

Fig. 4 The CD spectra of $[Ru(L^1(+))_2]^{2+}$ (a) and $[Ru(L^1(-))_2]^{2+}$ (b) in acetonitrile (1×10^{-5} M) and of $[Ru(trpy)(L^2(+))]^{2+}$ (c) and $[Ru(trpy)(L^2(-))]^{2+}$ (d) in Tris buffer.

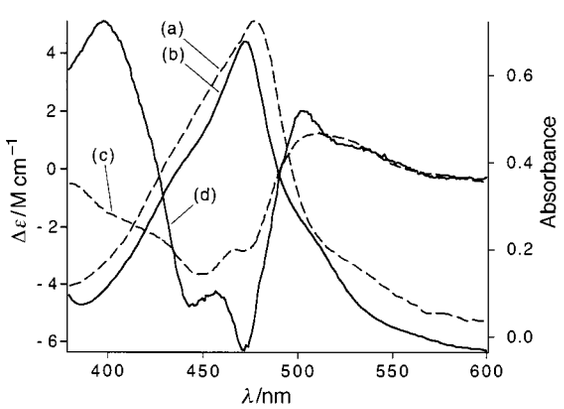

Fig. 5 Absorption (a,b) and circular dichroism spectra (c,d) of the MLCT transition of $[Ru(trpy)(L^1(-))]^{2+}$ (dashed line) and $[Ru(L^1(-))_2]^{2+}$ (full line) in acetonitrile (2×10^{-4} M).

transitions are observed for the ruthenium complexes at around 450 nm. The absorption spectra of $L^1(-)$, $[Ru(trpy)_2]^{2+}$, $[Ru(trpy)(L^1(-))]^{2+}$ and $[Ru(L^1(-))_2]^{2+}$ (Fig. 2) show components in the ligand centered absorptions which can be attributed to short and long axis polarized $\pi \longrightarrow \pi^*$ transitions. For $L^1(-)$ C_2 symmetry, the long axis transition transforms as A, the short axis transition as B, in trpy as A_1 and B_1, respectively.

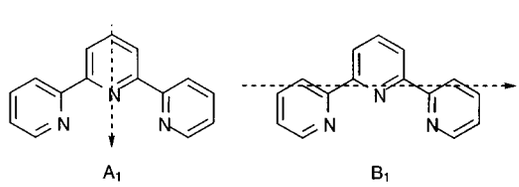

ZINDO Calculations (INDO/1 parameterization,[27] active space for singlet/triplet CI within 38 orbitals lying below and above the HOMO/LUMO pair) indicate that the lowest lying

Table 3 Calculated *versus* experimental transitions for trpy and $L^1(-)$. The main single determinants after CI are listed in brackets

	Trpy		$L^1(-)$	
	Calc. (λ/nm, f[a])	Measured (λ/nm, ε/M^{-1} cm^{-1})	Calc. (λ/nm, f[a])	Measured (λ/nm, ε/M^{-1} cm^{-1})
Short-axis polarized	215 (0.32) $\lvert^1A_1;a_2(\pi) \longrightarrow a_2(\pi^*)\rangle$	236 (38400)	297 (0.52) $\lvert^1A_1;a_2(\pi) \longrightarrow a_2(\pi^*)\rangle$	289 (sh) 300 (55000)
Long-axis polarized	274 (0.29) $\lvert^1B_1;a_2(\pi) \longrightarrow b_2(\pi^*)\rangle$	260 (20200)	266 (0.58) $\lvert^1B_1;b_2(\pi) \longrightarrow a_2(\pi^*)\rangle$	278 (45000) 258 (34000)
Long-axis polarized			315 (0.45) $\lvert^1B_1;a_2(\pi) \longrightarrow b_2(\pi^*)\rangle$	296 (52000) 318 (sh)

[a] f is oscillator strength.

Table 4 Possible MLCT and LC transitions in for a D_{2d} symmetrical d^6 complex

$[Ru(trpy)_2]^{2+}$	Transitions	Corresponding states	Transitions	Corresponding states
MLCT	$b_2 \longrightarrow b_1$	$A_1 \longrightarrow A_2$	$e \longrightarrow b_1$	$A_1 \longrightarrow E$
	$b_2 \longrightarrow e$	$A_1 \longrightarrow E$	$e \longrightarrow e$	$A_1 \longrightarrow A_1$, A_2, B_1, B_2
	$b_2 \longrightarrow a_2$	$A_1 \longrightarrow B_1$	$e \longrightarrow a_2$	$A_1 \longrightarrow E$
LC	$a_2 \longrightarrow e$	$A_1 \longrightarrow E$	$b_1 \longrightarrow a_2$	$A_1 \longrightarrow B_2$
	$a_2 \longrightarrow b_1$	$A_1 \longrightarrow B_2$	$e \longrightarrow e$	$A_1 \longrightarrow A_1$, A_2, B_1, B_2
	$a_2 \longrightarrow a_2$	$A_1 \longrightarrow A_1$	$e \longrightarrow b_1$	$A_1 \longrightarrow E$
	$b_1 \longrightarrow e$	$A_1 \longrightarrow E$	$e \longrightarrow a_2$	$A_1 \longrightarrow E$
	$b_1 \longrightarrow b_1$	$A_1 \longrightarrow A_1$		

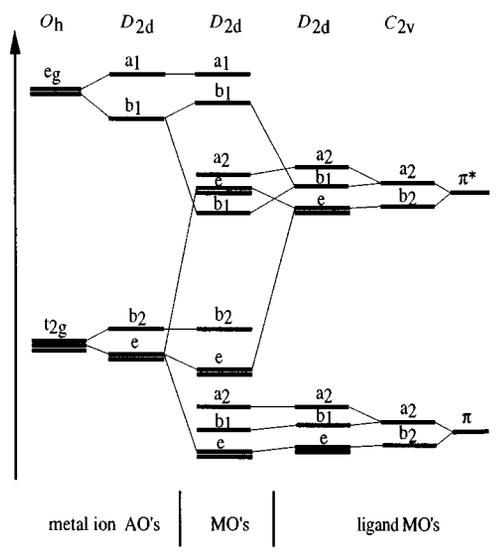

Fig. 6 Qualitative MO scheme of $[Ru(trpy)_2]^{2+}$ (D_{2d}) and trpy (C_{2v}).

$\pi \longrightarrow \pi^*$ transitions [260 nm for trpy, 296 nm for $L^1(-)$] are long axis polarized (Table 3). The corresponding MO scheme of $[Ru(trpy)_2]^{2+}$ is depicted in Fig. 6. For all metal complexes the LC transitions are shifted to lower energy as compared to those of 'free;' ligand due the positive charge of the central metal, which increases the energy of the lowest π orbital of the ligand. This behavior was also observed for complexes of the tris-(bipyridyl) type.[28] The MLCT transitions carry large intensities if the electron flow is parallel to the electric dipole moment.[29] The electron flow during a MLCT transition is directed along the S_4 axis (z axis) which transforms as B_2. Therefore, the most intense MLCT transition is attributed to $\lvert^1B_2;e(d_{xy},d_{yz}) \longrightarrow e(\pi^*)\rangle$.[30,31] Emission properties have not been investigated in detail. At room temperature no emission is detectable as the excited state lifetimes of ruthenium(II) bis(terpyridyl) complexes are expected to be very short, *i.e.* for $[Ru(trpy)_2]^{2+}$ $\tau = 250$ ps in water.[32]

CD Spectra

Cotton effects can be conveniently classified into three types by considering the symmetry properties and the nature of the chromophores and their transitions: (I) from inherently achiral chromophores which are asymmetrically perturbed; (II) from inherently chiral chromophores; (III) due to dipole–dipole interactions between more than two chromophores, the orbitals of which do not mutually overlap. The amplitudes of Cotton effects of type I are usually very small. Free L^1 or L^2 is such a case where a chiral substituent imposes a dissymmetric environment. The CD spectrum of $L^1(-)$ [Fig. 3(a)] is similar to those of (+)-α-pinene and other pyridines with pinene groups attached.[12] However in the case of the reported complexes with L^1, stronger CD in the LC absorptions indicates that effects of type II or III must be present (Fig. 3). All enantiomeric pairs show mirror image CD as exemplified in Fig. 4. As crystal structure analyses of $[Rh(L^1(-))Cl_3]$ and $[Ru(L^1(-))Cl_3]$ show (Fig. 7), a helical distortion of the ligand π system occurs upon complexation, which is less pronounced in the complex $[Ru(trpy)(L^2(-))][PF_6]$. (Fig. 8). In free L^1 the pyridyl moieties have a low energy barrier for rotation around the 2,2′ and 2′,6″ bonds, whereas upon complexation rotation is excluded and the ligand is forced to take a helically distorted geometry. As a result of this helicity, all MLCT transitions show significant CD, which would not be present if the two ligand π systems were planar and strictly perpendicular (even though with chiral substituents) to each other. The sign of the CD bands of MLCT transitions can be derived from symmetry consideration of the orbitals involved. The condition to observe for rotational strength is $\langle a|\vec{\mu}|b\rangle\langle a|\vec{m}|b\rangle \neq 0$. The z-axis directed MLCT transition in D_{2d} $\lvert^1B_2;e(d_{xy},d_{yz}) \longrightarrow e(\pi^*)\rangle$ that carries most intensity becomes $\lvert^1B_1;b(d_{xy,yz}) \longrightarrow b(\pi^*)\rangle$ in D_2 and $\lvert^1A;b(d_{xy,yz}) \longrightarrow b(\pi^*)\rangle$ in C_2, respectively, and in both cases transforms as R_z. Therefore these transitions also have non-zero rotational strengths. The sign of the CD of z-axis polarized transitions being only a function of the helicity of the π orbital involved, one finds that a left handed helical arrangement as in the crystal structure of $[Ru(L^1(-))Cl_3]$ (Fig. 7) leads to a left handed charge displacement corresponding to a negative CD. This is observed for the strongest MLCT transitions of these complexes, which are therefore tentatively assigned to $\lvert^1B_1;b((d_{xz,yz}) \longrightarrow b(\pi^*)\rangle$ (Fig. 5). The CD activity in the LC transitions of bis(terpyridyl) complexes (Fig. 3) mainly arise from exciton coupling[33] between two intraligand transitions or between two different terpyridyl ligands which have non-orthogonal transition dipole moments due to the out of plane distortion of the terpyridyl moiety. From the CD and UV-VIS

spectra the exciton splitting is determined to be around 1000 cm^{-1} for the long axis polarized transition at around 315 nm (Fig. 3) of $[Ru(L^2)_2]^{2+}$. The observed Cotton effect is consistent with a ligand geometry as found in $[Ru(L^1(+))Cl_3]$ (Fig. 7). As the terpyridyl ligand L^2 is somewhat less distorted in the ruthenium complexes than is the ligand L^1, CD values recorded for $[Ru(L^2)_2]^{2+}$ and $[Ru(trpy)(L^2)]^{2+}$ (Fig. 4) are smaller than those of $[Ru(L^1)_2]^{2+}$ and $[Ru(trpy)(L^1)]^{2+}$. Therefore, we conclude that the transitions observed are due to the intrinsic helical arrangement of the ligand fixed at a metal center.

Cyclic voltammetry

In comparison to $[Ru(trpy)_2]^{2+}$, the oxidation potentials of $[Ru(trpy)(L^1(-))]^{2+}$ and $[Ru(L^1(-))_2]^{2+}$ are slightly increased (Table 5). It is also evident that the first reduction in $[Ru(trpy)(L^1(-))]^{2+}$ occurs in the trpy moiety since its reduction potential is equivalent to that of $[Ru(trpy)_2]^{2+}$. The ligand $L^1(-)$ is a slightly weaker π^* acceptor with respect to trpy and it has therefore a slightly lower reduction potential.

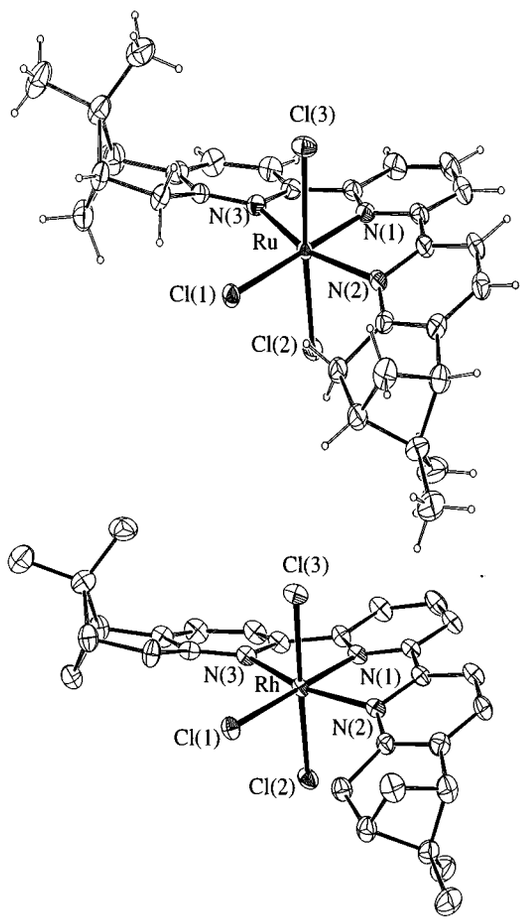

Fig. 7 Molecular views of $[Ru(L^1(-))Cl_3]$ (with hydrogens) and $[Rh(L^1(-))Cl_3]$ (without hydrogens) with 50% probability thermal ellipsoids depicted.

Crystallographic data

Selected bond lengths, angles and dihedral angles of $[Rh(L^1(-))Cl_3]$ and $[Ru(L^1(-))Cl_3]$ are given in Table 7, lengths and angles of $[Ru(trpy)(L^2(-))][PF_6]_2$ in Table 8.

The molecular structures of $[Rh(L^1(-))Cl_3]$ and $[Ru(L^1(-))Cl_3]$ are shown in Fig. 7. The helical out of plane distortion of the terpyridyl moiety is evident. The twisting angle between the two distant pyridine rings is 32 and 31° for the two complexes and the absolute configuration of these two rings can be denoted as Λ using the IUPAC designation for a pair of skew lines.

The molecular structures of $L^2(-)$ and $[Ru(trpy)(L^2(-))]Cl_2$ with the atom numbering schemes are shown in Fig. 8. That of $L^2(-)$ possesses a twofold axis relating two asymmetric units through N(1) and C(3). The main part of the molecule is planar with the largest deviation being 0.168 Å at N(1). Only the C atoms of the pinene fragment are out of the plane with C(11) and C(13) being away from it by 1.13 and −1.10 Å. The cation $[Ru(trpy)(L^2(-))]^{2+}$ adopts a six-co-ordinate geometry with a *mer* conformation of the two terpyridyl ligands which make a dihedral angle of 95.2°. The distances between Ru and the central N(1) or N(4) atoms, 1.982(6) and 1.957(6) Å respectively, are significantly shorter than the values observed for the other Ru–N bonds, 2.065 Å (mean), and are comparable with the distances in $[Ru(L^1(-))Cl_3]$.

Conclusion

Mono- or bis- 2,2′;6′,6″-terpyridyl complexes of octahedral co-ordination centers have often been considered to be valuable alternatives to bis- or tris-diimine complexes, because the problem of chirality, leading to isomeric mixtures in synthesis, can be avoided. This is due to the fact that terpyridyl ligands can co-ordinate exclusively in a meridional way in an

Table 5 Electrochemical data for $[Ru(trpy)_2]^{2+}$, $[Ru(trpy)(L^1(-))]^{2+}$ and $[Ru(L^1(-))_2]^{2+}$

Complex	E_0/V	$E_1/\Delta E$	E_2/V	I_a/I_c
$[Ru(trpy)_2]^{2+}$	1.28 (0.09)	−1.27 (0.08)	−1.52 (0.10)	0.98
$[Ru(trpy)(L^1(-))]^{2+}$	1.31 (0.10)	−1.26 (0.08)	−1.64 (0.10)	0.95
$[Ru(L^1(-))_2]^{2+}$	1.34 (0.10)	−1.37 (0.08)	−1.67 (0.10)	0.85

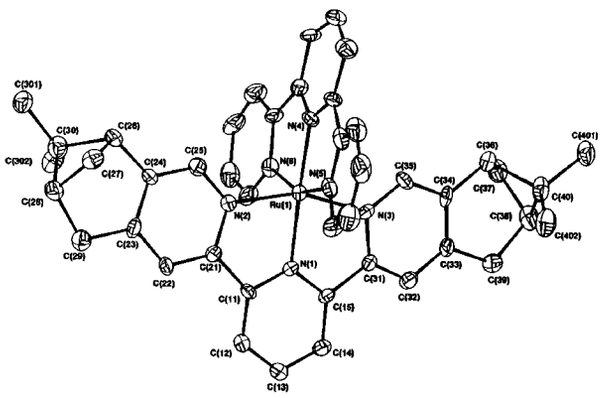

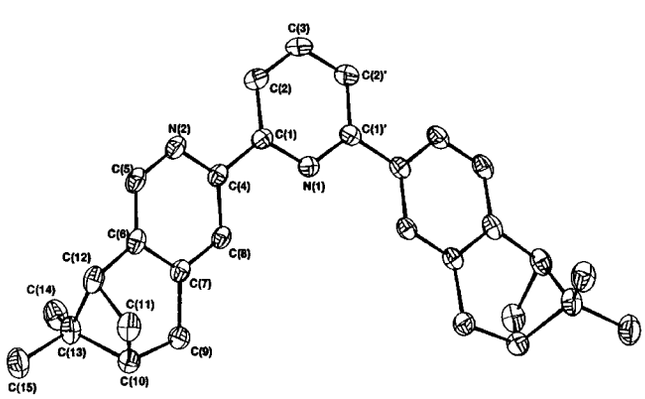

Fig. 8 Molecular views of $L^2(-)$ and $[Ru(trpy)(L^2(-))][PF_6]_2$ with 30% probability thermal ellipsoids depicted.

Table 6 Crystallographic data of $L^2(-)$, $[Ru(trpy)(L^2(-))][PF_6]_2$ **8a**, $[Ru(L^1(-))Cl_3]$ **2** and $[Rh(L^1(-))Cl_3]$ **3**

	$L^2(-)$	**8a**	**2**	**3**
Molecular formula	$C_{29}H_{31}N_3$	$C_{44}H_{42}F_{12}N_6P_2Ru$	$C_{32}H_{37}Cl_3N_3ORu$	$C_{29}H_{31}Cl_3N_3Rh$
Molecular weight	421.63	1045.91	687.10	630.85
Crystal system	Orthorhombic	Orthorhombic	Orthorhombic	Orthorhombic
Space group	$P2_122_1$	$P2_12_12_1$	$P2_12_12_1$	$P2_12_12_1$
a/Å	6.5893(9)	9.508(1)	7.9867(7)	7.9810(10)
b/Å	9.080(1)	12.745(2)	15.6250(13)	15.571(2)
c/Å	19.494(4)	37.781(4)	25.199(2)	24.630(2)
V/Å^3	1167.0(2)	4578(1)	3144.6(4)	3060.8(6)
Z	2	4	4	4
T/K	293(2)	293(2)	180(2)	193(2)
μ/mm^{-1}	0.066	0.489	0.77	1.02
No. reflections measured	7285	16335	20175	3075
No. unique reflections	1783	4800	4945	3072
R_{int}	0.032	0.059	0.0431	0
Flack's parameter		0.03(5)	−0.03(4)	−0.05(5)
Final R values	$R(F) = 0.0363$	$R(F) = 0.0440$	$R(F) = 0.0217$	$R(F^2) = 0.0396$
	$wR(F) = 0.0317$	$wR(F = 0.0499$	$wR(F) = 0.0244$	$wR(F^2) = 0.1020$
Goodness of fit	1.054	1.130	1.063	1.101

Table 7 Selected bond lengths (Å), angles and angles between the planes of the pyridyl moieties (°) for $[Rh(L^1(-))Cl_3]$ and $[Ru(L^1(-))Cl_3]$ where P2 and P3 denote the outer pyridine ring with N(2) and N(3) respectively, P1 the central pyridine ring with N(1)

	$[Ru(L^1(-))Cl_3]$	$[Ru(L^1(-))Cl_3]$
M–Cl(1)	2.3729(14)	2.3794(6)
M–Cl(2)	2.3331(16)	2.3322(7)
M–Cl(3)	2.3365(16)	2.3504(7)
M–N(1)	1.942(5)	1.967(2)
M–N(2)	2.110(5)	2.147(2)
M–N(3)	2.111(5)	2.139(2)
Cl(1)–M–Cl(2)	91.09(6)	93.04(2)
Cl(1)–M–Cl(3)	92.00(6)	92.29(2)
Cl(1)–M–N(1)	179.66(16)	179.70(6)
Cl(1)–M–N(2)	99.89(14)	100.78(6)
Cl–M–N(3)	100.03(15)	100.37(6)
Cl(2)–M–Cl(3)	176.82(6)	174.66(3)
Cl(2)–M–N(1)	88.74(16)	86.85(6)
Cl(2)–M–N(2)	89.86(14)	89.64(6)
Cl(2)–M–N(3)	88.97(14)	89.05(6)
Cl(3)–M–N(1)	88.17(16)	87.82(6)
Cl(3)–M–N(2)	90.30(14)	89.14(6)
Cl(3)–M–N(3)	89.80(14)	90.21(6)
N(1)–M–N(2)	79.82(21)	79.51(9)
N(1)–M–N(3)	80.25(21)	79.34(9)
N(2)–M–N(3)	160.07(20)	158.85(8)
P1/P2	14.9(3)	18.85(13)
P1/P3	18.8(3)	13.08(13)
P2/P3	32.0(3)	30.72(13)

Table 8 Interatomic distances (Å) and angles (°) for $[Ru(trpy)(L^2(-))][PF_6]_2$

Ru(1)–N(1)	1.982(6)	Ru(1)–N(4)	1.957(6)
Ru(1)–N(2)	2.066(6)	Ru(1)–N(5)	2.073(7)
Ru(1)–N(3)	2.064(6)	Ru(1)–N(6)	2.057(6)
N(1)–Ru(1)–N(2)	78.7(3)	N(3)–Ru(1)–N(5)	95.5(2)
N(1)–Ru(1)–N(3)	79.7(3)	N(4)–Ru(1)–N(5)	79.0(3)
N(2)–Ru(1)–N(3)	158.4(3)	N(1)–Ru(1)–N(6)	101.0(3)
N(1)–Ru(1)–N(4)	177.5(3)	N(2)–Ru(1)–N(6)	92.9(2)
N(2)–Ru(1)–N(4)	103.9(3)	N(3)–Ru(1)–N(6)	90.3(3)
N(3)–Ru(1)–N(4)	97.7(2)	N(4)–Ru(1)–N(6)	79.0(3)
N(1)–Ru(1)–N(5)	101.0(3)	N(5)–Ru(1)–N(6)	157.9(3)
N(2)–Ru(1)–N(5)	89.4(2)		

octahedral complex. Monoterpyridyl complexes therefore have inherently C_{2v} symmetry, bis(terpyridyl) complexes D_{2d}, both achiral symmetry groups. The chiral terpyridyl ligands that are introduced here reduce these symmetries to C_2 and D_2, respectively (at least for the bis-homochiral terpyridine complex). Since the synthesis of the chiral terpyridyl ligands, derived from that of the earlier published and very versatile method for bipyridine derivatives, yields enantiopure material from natural products, the problem of isomeric mixtures does not occur any more, even though the resulting complexes are chiral. This fact adds a new dimension to the chemistry of octahedral complexes with terpyridyl ligands. For chiral structures, additional spectroscopic information is available from CD spectra. There is also a possibility to study interactions of such complexes with other chiral structures and finally there might be the possibility to build up relatively large linear structures that have a "chiral twist". The introduction of the chiralized terpyridyl ligands, opens up the already quite varied chemistry of terpyridyl complexes using these ligands which introduce a well defined chiral element.

Acknowledgements

We thank Dominique Suhr for assistance in the synthesis of ligand $L^1(+)$, Dr Catherine Verchère-Béaur for measuring CD spectra of $[Ru(trpy)(L^2)]Cl_2$, Professor Peter Belser for advice concerning the synthesis of ruthenium complexes, and Professor R. Chauvin for fruitful discussion. The Swiss National Science Foundation and the Centre National de la Recherche Scientifique are acknowledged for financial support.

References

1 J.-P. Collin, P. Gavina, V. Heitz and J.-P. Sauvage, *Eur. J. Inorg. Chem.*, 1998, **1**, 1.
2 E. C. Constable and A. W. C. Thompson, *J. Chem. Soc.*, *Dalton Trans.*, 1992, 2947.
3 J. P. Collin, S. Guillerez, J. P. Sauvage, F. Barigelletti, L. D. Cola, L. Flamigni and V. Balzani, *Inorg. Chem.*, 1991, **30**, 4230.
4 B. J. Coe, D. W. Thomson, C. T. Culbertson, J. R. Schoonover and T. J. Meyer, *Inorg. Chem.*, 1995, **34**, 3385.
5 D. J. Cardenas, P. Gavina and J. P. Sauvage, *Chem. Commun.*, 1996, 1915.
6 G. S. Hanan, C. R. Arana, J. M. Lehn, G. Baum and D. Fenske, *Chem. Eur. J.*, 1996, **2**, 1292.
7 L. M. Scolaro, A. Romeo and A. Terracina, *Chem. Commun.*, 1997, 1451.
8 V. Grosshenny, A. Harriman, M. Hissler and R. Ziessel, *Platinum Metals Rev.*, 1996, **40**, 72.
9 F. Barigelletti, L. Flamigni, V. Balzani, J.-P. Collin, J.-P. Sauvage and A. Sour, *New J. Chem.*, 1995, **19**, 793.
10 H. M. Brothers and N. M. Kostic, *Inorg. Chem.*, 1988, **27**, 1761.

11 H. Shirai, K. Hanabusa, Y. Takahashi, F. Mizobe and K. Hanada, *PCT Int. Appl.*, WO 94 14440 (Cl. A61K31/44), 7 July 1994, JP Appl. 92/348, 684, 28 Dec 1992, (*Chem. Abstr.*, 121: 195935f).
12 N. C. Fletcher, F. R. Keene, M. Ziegler, H. Stoeckli-Evans, H. Viebrock and A. Von Zelewsky, *Helv. Chim. Acta*, 1996, **79**, 1192.
13 H. Mürner, P. Belser and A. Von Zelewsky, *J. Am. Chem. Soc.*, 1996, **118**, 7989.
14 H. Mürner, G. Hopfgartner and A. Von Zelewsky, *Inorg. Chim. Acta*, 1998, **271**, 36.
15 P. Hayoz, A. Von Zelewsky and H. Stoeckli-Evans, *J. Am. Chem. Soc.*, 1993, **115**, 5111.
16 E. C. Constable, T. Kulke, M. Neuburger and M. Zehnder, *Chem. Commun.*, 1997, 489.
17 (*a*) R. Glaser, *Chirality*, 1993, **5**, 272; (*b*) A. Horeau, personal communication and Collège de France lectures; (*c*) K. Mislow, *Bull. Soc. Chim. Fr.*, 1994, **131**, 534.
18 B. P. Sullivan, J. M. Calvert and T. J. Meyer, *Inorg. Chem.*, 1980, **19**, 1404.
19 E. C. Constable, *J. Chem. Soc.*, *Dalton Trans.*, 1985, 2687.
20 E. D. Mihelich and D. J. Eickhoff, *J. Org. Chem.*, 1983, **48**, 4135.
21 R. K. De Richter, M. Bonato, M. Follet and K. Jean-Marc, *J. Org. Chem.*, 1990, **55**, 2855.
22 F. Kröhnke, *Synthesis*, 1976, 1.
23 D. Rose and G. Wilkinson, *J. Chem. Soc., A.*, 1970, 1791.
24 T. J. Meyer and J. N. Braddock, *J. Am. Chem. Soc.*, 1973, **95**, 3158.
25 M. L. Stone and G. A. Crosby, *Chem. Phys. Lett.*, 1981, **79**, 169.
26 P. Hayoz and A. Von Zelewsky, *Tetrahedron Lett.*, 1992, **33**, 5165.
27 W. P. Anderson, T. R. Cundari, R. S. Drago and M. C. Zerner, *Inorg. Chem.*, 1990, **29**, 1.
28 I. Hanazaki and S. Nagakura, *Inorg. Chem.*, 1969, **8**, 648.
29 P. Day and N. J. Sanders, *J. Chem. Soc. A*, 1967, 1536.
30 C. Daul, C. W. Schlaepfer, A. Goursot, E. Penigault and J. Weber, *Chem. Phys. Lett.*, 1981, **78**, 304.
31 C. Daul and J. Weber, *Chem. Phys. Lett.*, 1981, **77**, 593.
32 J. R. Winkler, T. L. Netzel, C. Creutz and N. J. Sutin, *J. Am. Chem. Soc.*, 1987, **109**, 2381.
33 M. Ziegler and A. Von Zelewsky, *Chem. Coord. Rev.*, 1998, in the press.

Paper 9/00194H